Supporting Information

Experimental details

Methylammonmium iodide (CH_3NH_3I) synthesis: Methylammonmium iodide was synthesized using the method described by Lee *et al.*[1]. Methylamine (24 mL) was reacted with 10 mL of hydroiodic acid–ethanol solution at room temperature, and the crystallized methylammonmium iodide was separated by rotary evaporation.

Solution preparation: PbI_2–$PbCl_2$ DMF solution was prepared by mixing different molar ratios of $PbCl_2$ and PbI_2 (Table S1), dissolving in DMF, heating at 70 °C, and stirring overnight.

Table S1. PbI_2–$PbCl_2$ DMF solution preparation

$PbCl_2$ molar ratio	PbI_2 (mg)	$PbCl_2$ (mg)	DMF (mL)
0%	460	-	1
25%	345	69	1
33%	306	92	1
50%	230	139	1

CH_3NH_3I isopropanol solution was prepared by dissolving 40 mg CH_3NH_3I into 1 mL isopropanol.

Substrate preparation and perovskite solar cell fabrication: FTO glass was cleaned ultrasonically and sequentially with deionized water, acetone, and ethanol, followed by oxygen plasma treatment for 20 min. Compact TiO_2 precursor solution, which was prepared according to the method reported by Abrusci *et al.*[2], was spin-coated onto the cleaned FTO surface at of 2000 rpm for 45 s followed by annealing at 50 °C for 30 min. PbI_2–$PbCl_2$ DMF solution was spin-coated at 2000 rpm and 70 °C for 30 min and annealed at 100 °C for 60 min. CH_3NH_3I isopropanol solution was hot spin-coated onto the PbI_2–$PbCl_2$ film at 2000 rpm. Solvent annealing, which was reported by Xiao et. al.[3] was conducted for 60 min at 100 °C to form the perovskite film. Afterward, 72.3 mg of 2,2'.7.7'-tetrakis[*N*,*N*-di(4-methoxyphenyl)amino]=9,9'-spirobifluorene (Spiro-OMeTAD) dissolved in 1 mL of chlorobenzene precursor solution was spin-coated on the substrate at 2000 rpm for 60 min as a hole-transporting layer. Chlorobenzene precursor was prepared by adopting the method of Burschka *et al.*[4], in which 28.8 μL of 4-*tert*-butyl pyridine and 17.5 μL of 520 mg/mL bis(trifluoromethylsulfonyl)imide acetonitrile stock solution was added to 1 mL of chlorobenzene. Finally, 75 nm of gold deposited by magnetron sputtering was selected as the counter electrode.

Characterization of PbI_2/$PbCl_2$ and perovskite films: PbI_2/$PbCl_2$ and perovskite films were characterized using UV-vis spectroscopy, SEM, and XRD at ambient conditions. The samples were prepared on the FTO with a compact TiO_2 layer and preserved in a glove box before the test because exposure to oxygen and moisture may change the properties of the samples. The UV absorption spectra of the samples were obtained using a Lambda 35 UV spectrometer (Perkin Elmer). The crystalline structures of the samples were determined using a one-dimensional X-ray diffractometer (X'pert Pro, Philips). Time-resolved photoluminescence measurements were obtained using a LifeSpec Red spectrometer (LifeSpec-Red, Edinburgh Inc.). The wavelength of the photoexcitation laser was 440 nm, and the detection wavelength was 780 nm. The test samples were prepared on glass. The morphology of the films was observed using a field emission scanning electron microscope (S-4800 Hitachi, Japan).

Solar cell characterization: The performance of planar heterojunction solar cells was determined at ambient conditions on a Keithley Model 2000 instrument under simulated AM 1.5 sunlight generated by a YSS-5A system (Yamashita DESO, Japan). Light intensity was calibrated to 100 mW/cm^2 by a standard silicon solar cell, and the active area of the solar cell was 3.14 mm^2. Scanning electron micrographs of the cross-section of the devices were also obtained by a field emission scanning electron microscope (S-4800 Hitachi, Japan). IPCE was obtained by a solar cell monochromatic incident photon-to-electron conversion efficiency measurement system (SCS10-X150-DSSC, Zolix); here, the active area of the test samples was 6 mm^2.

Table S2. Biexponential fit decay parameters for the photoluminescence decays shown in Figure 2d

$PbCl_2$ molar ratio	**0%**	**25%**	**33%**	**50%**
τ_{fast} **(ns)**	4.82	8.32	9.42	14.13
τ_{slow} **(ns)**	75.17	126.01	172.63	94.99
χ^2	1.217	1.07	0.995	1.134

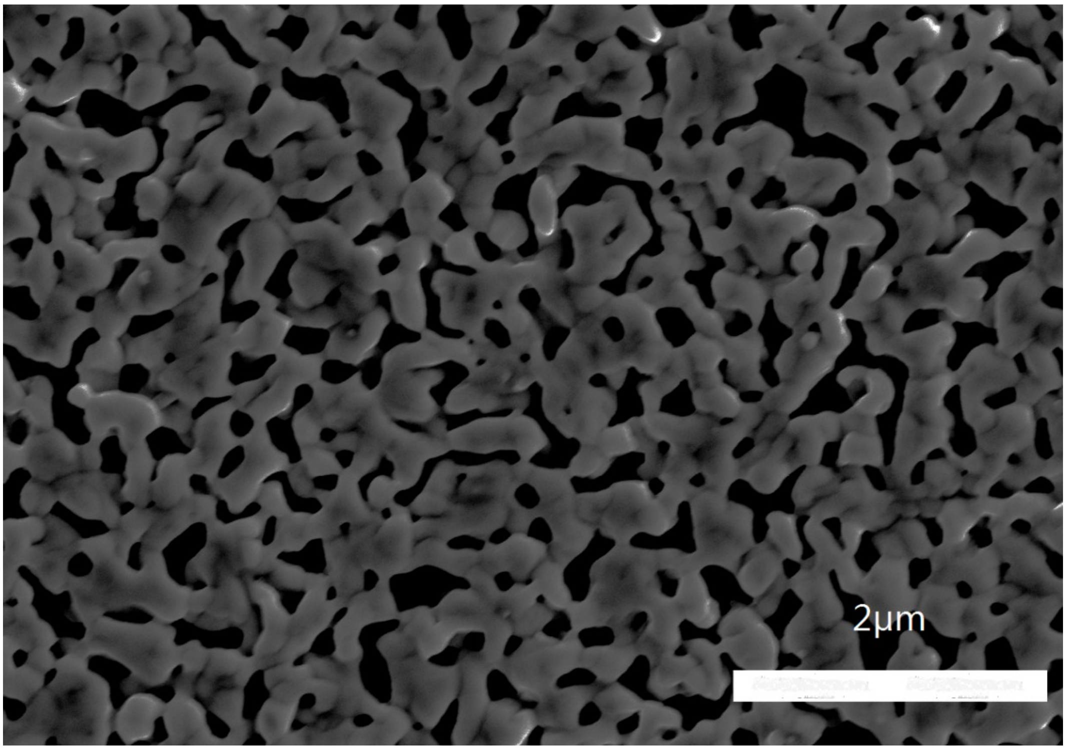

Figure S1 Scanning electron micrograph of a 33% $PbCl_2$ molar ratio $PbI_2/PbCl_2$ film spin-coated at room temperature (approximately 20 °C)

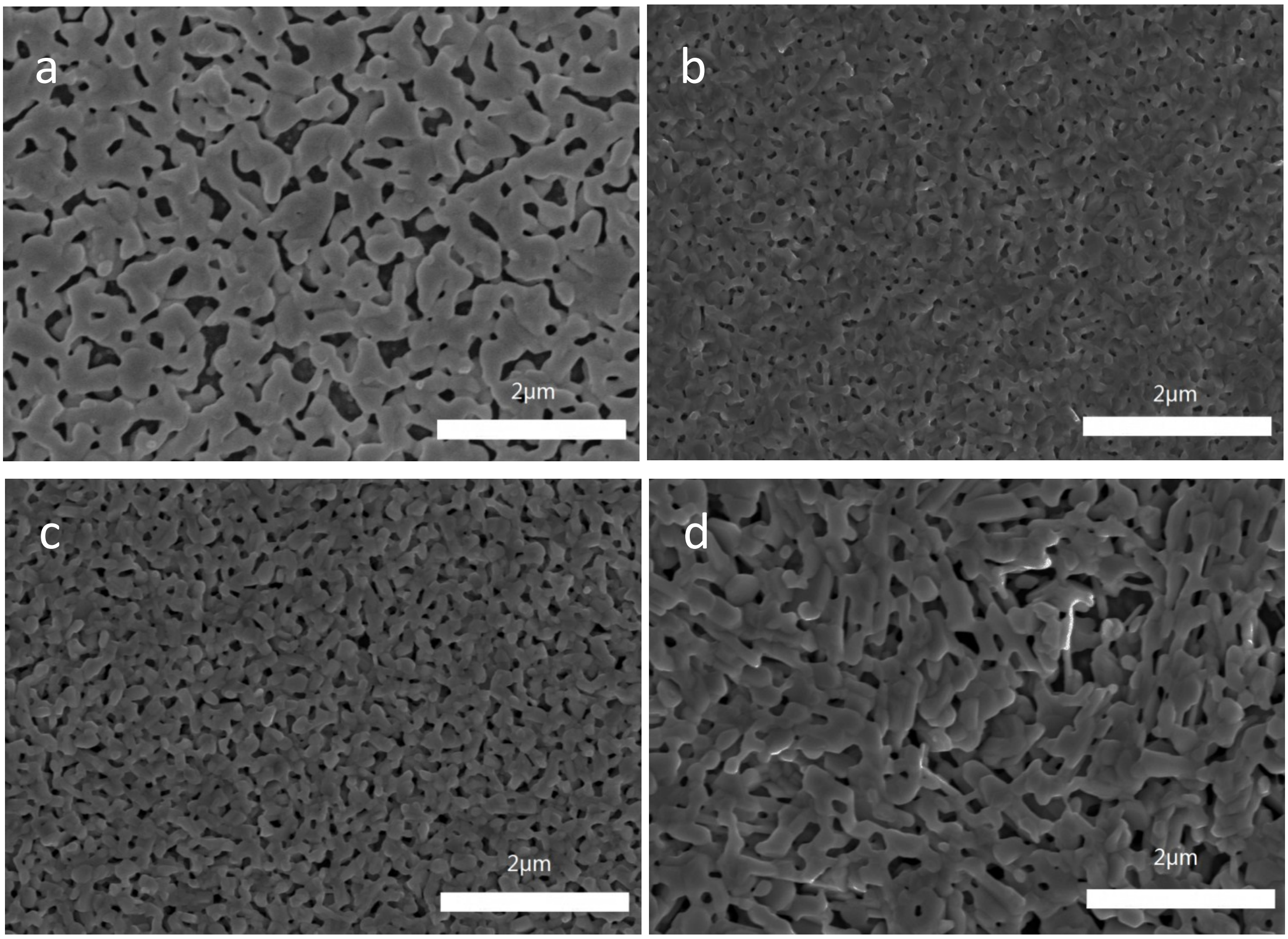

Figure S2 Scanning electron micrographs of $PbI_2/PbCl_2$ films based on different $PbCl_2$ molar ratios: (a) 50%, (b) 33%, (c) 25%, and (d) 0%

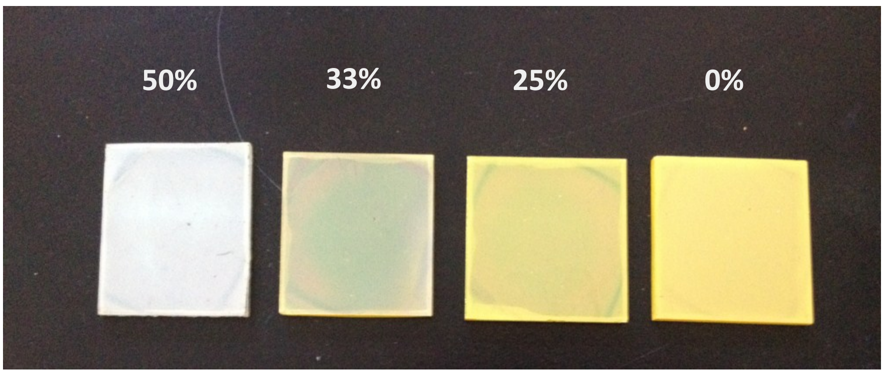

Figure S3 Photographs of $PbI_2/PbCl_2$ films with different $PbCl_2$ molar ratios

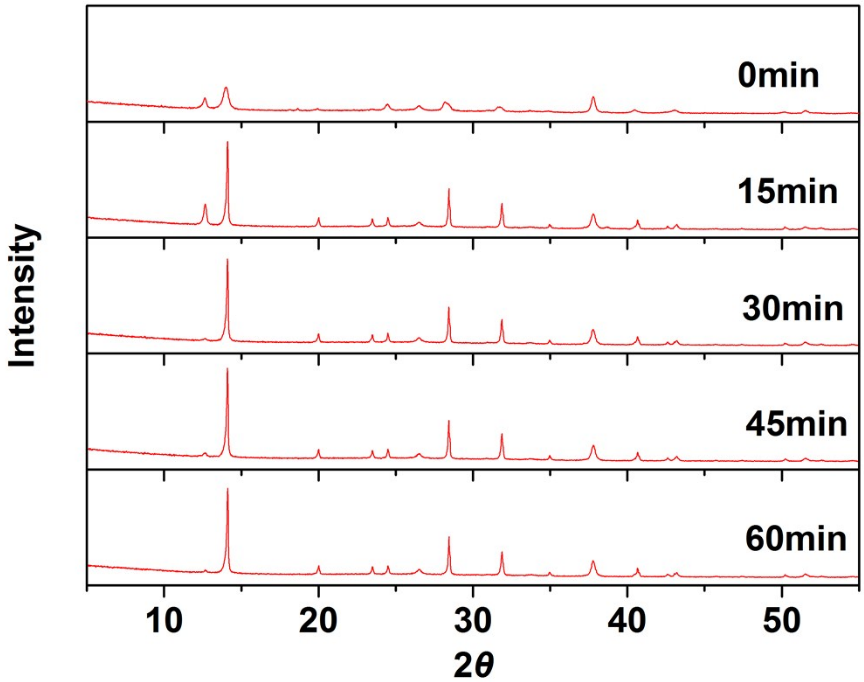

Figure S4 XRD patterns of perovskite films obtained from pure PbI_2 film samples with different annealing times

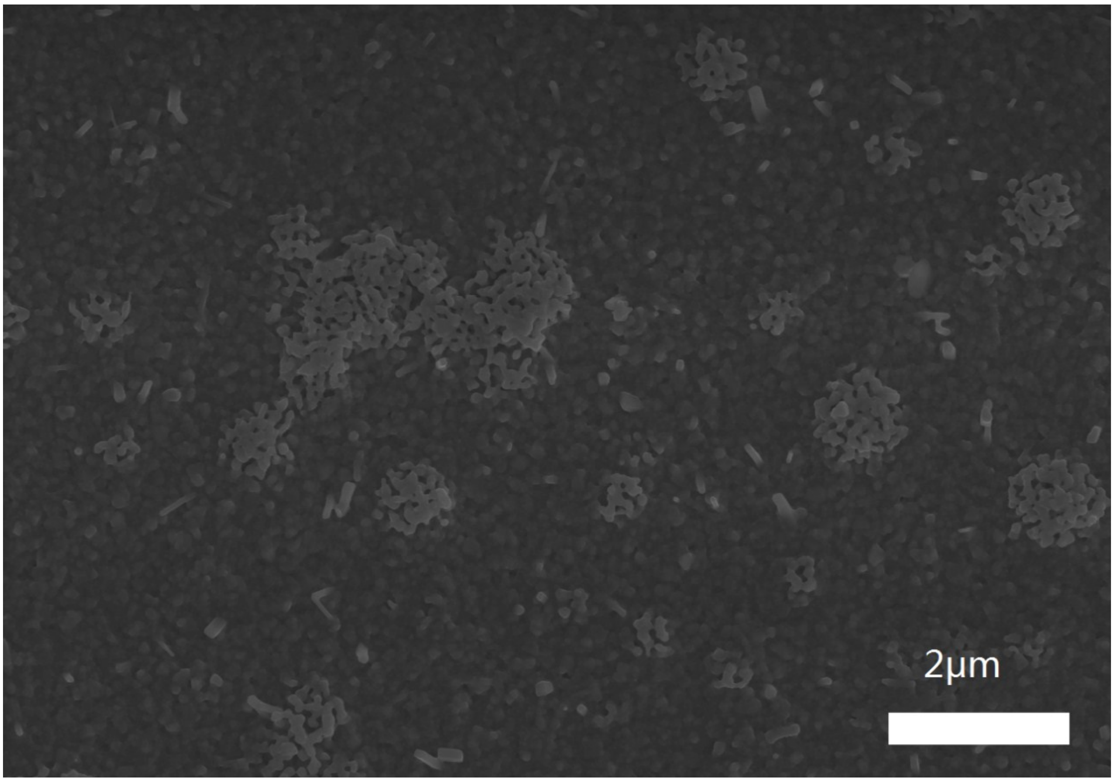

Figure S5 Scanning electron micrograph of 33% $PbCl_2$ molar ratio $PbI_2/PbCl_2$ film spin-coated CH_3NH_3I solution without annealing treatment

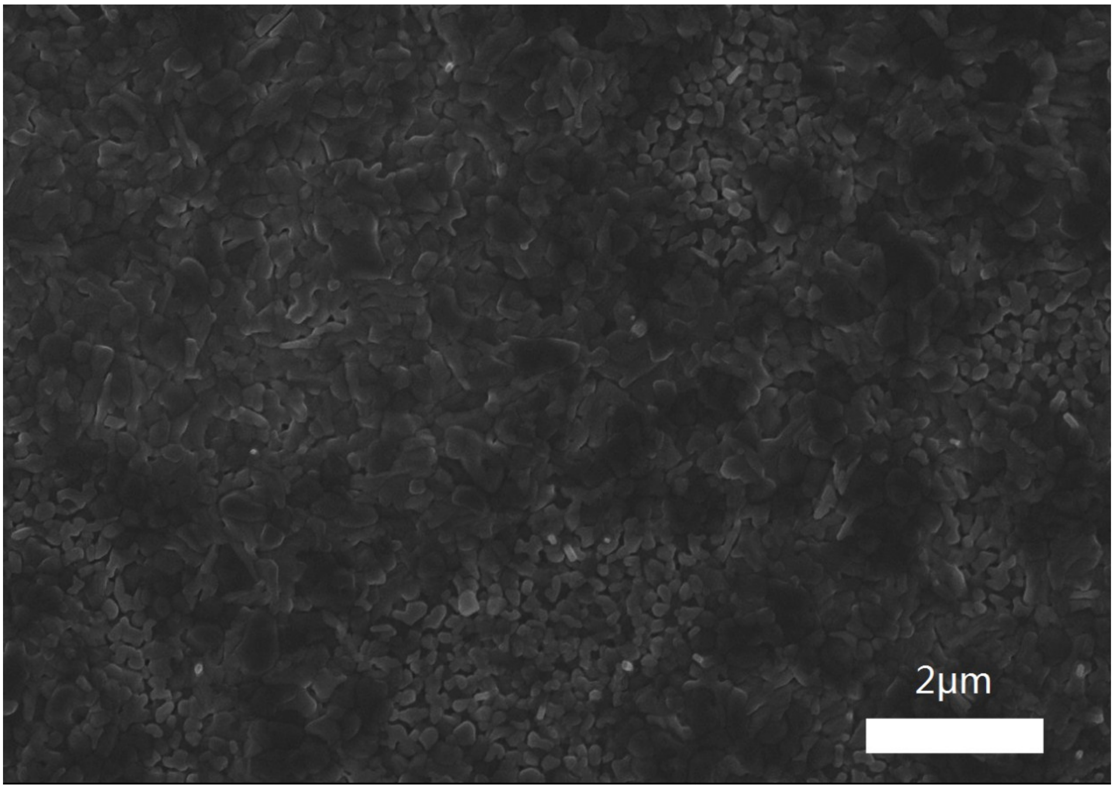

Figure S6 Scanning electron micrograph of 33% $PbCl_2$ molar ratio $PbI_2/PbCl_2$ film spin-coated CH_3NH_3I solution with thermal annealing treatment

Phase Sum Spectrum

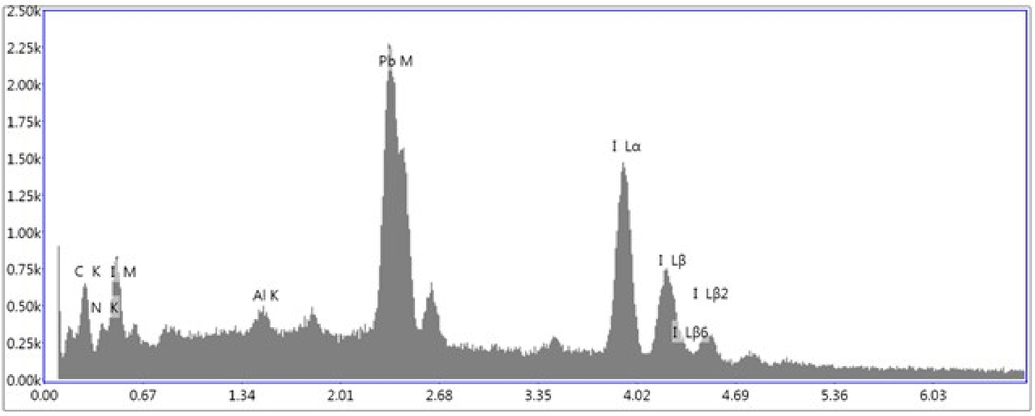

Element	Weight (%)	Atom (%)	Error(%)
C	4.56	31.98	8.28
N	2.31	13.87	12.55
Al	0.1	0.32	68.74
Pb	30.7	12.48	4.77
I	62.33	41.35	6.16

Figure S7 EDX characterization of perovskite based on 33% $PbCl_2$ molar ratio $PbI_2/PbCl_2$ film. The signal of Al may have originated from the sample stage.

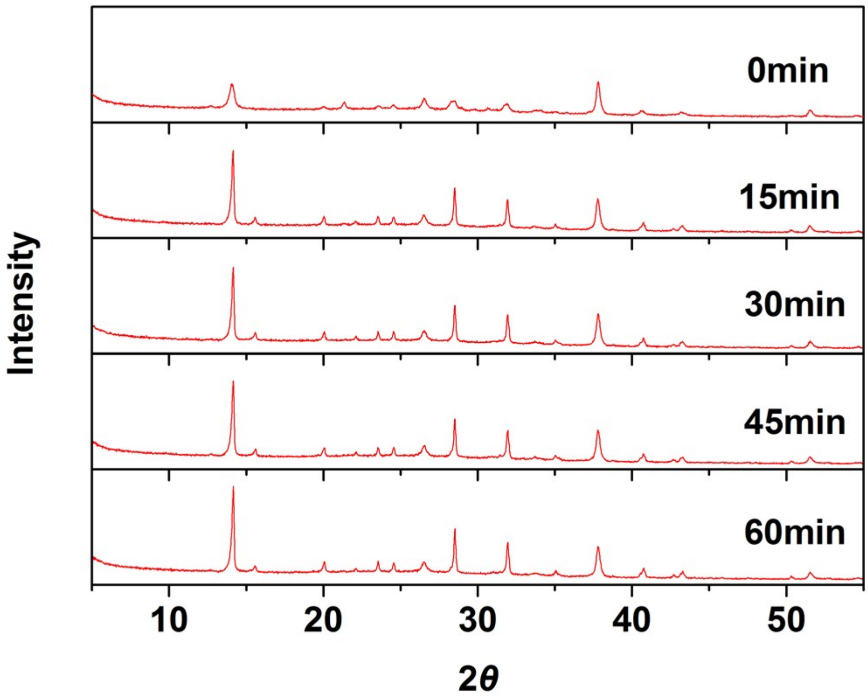

Figure S8 XRD patterns of perovskite films obtained from 33% $PbCl_2$ molar ratio $PbI_2/PbCl_2$ films featuring a spin-coating temperature of 30 °C and different annealing times

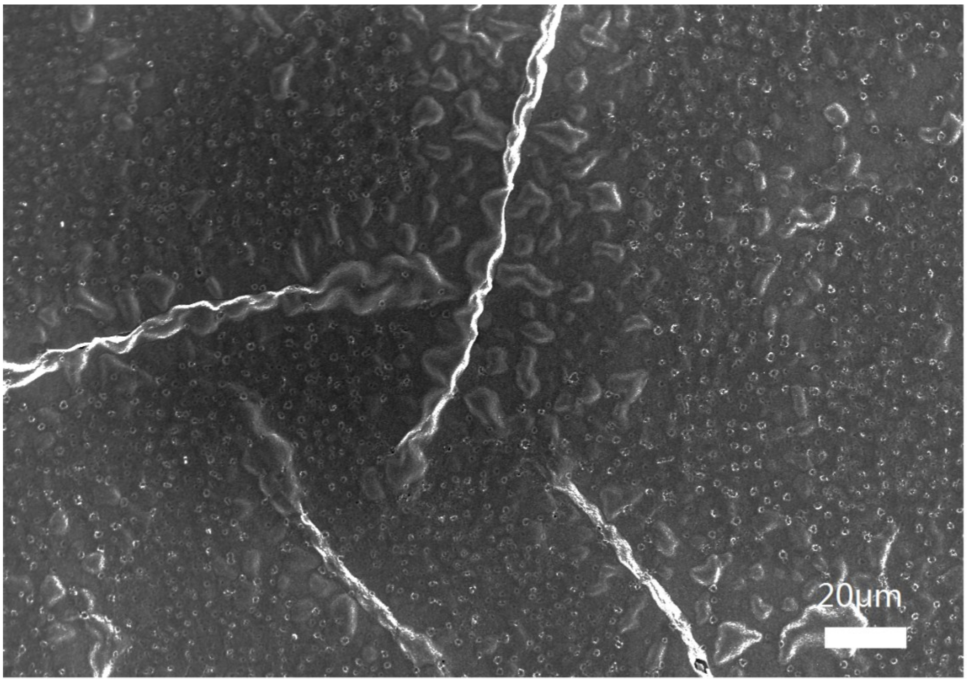

Figure S9 Scanning electron micrograph of surface damage on 33% $PbCl_2$ molar ratio $PbI_2/PbCl_2$ film spin-coated CH_3NH_3I solution at 60 °C

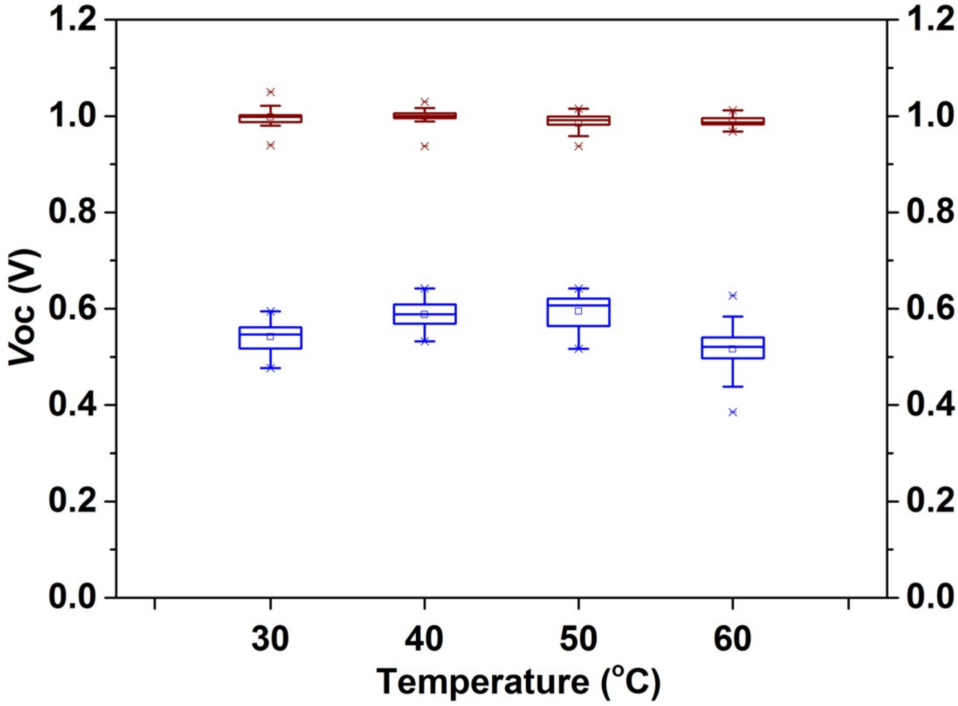

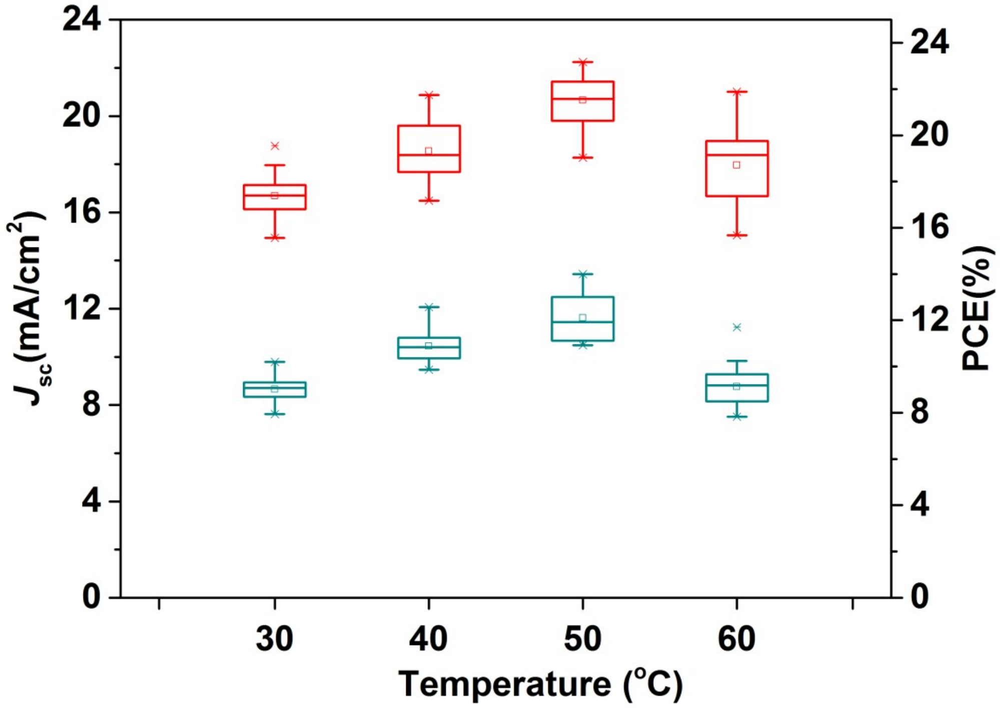

Figure S10 Photovoltaic parameters of perovskite solar cells based on pure PbI_2 prepared at different CH_3NH_3I spin-coating temperatures. Each box presents the parameter distribution of 40 devices under similar conditions.

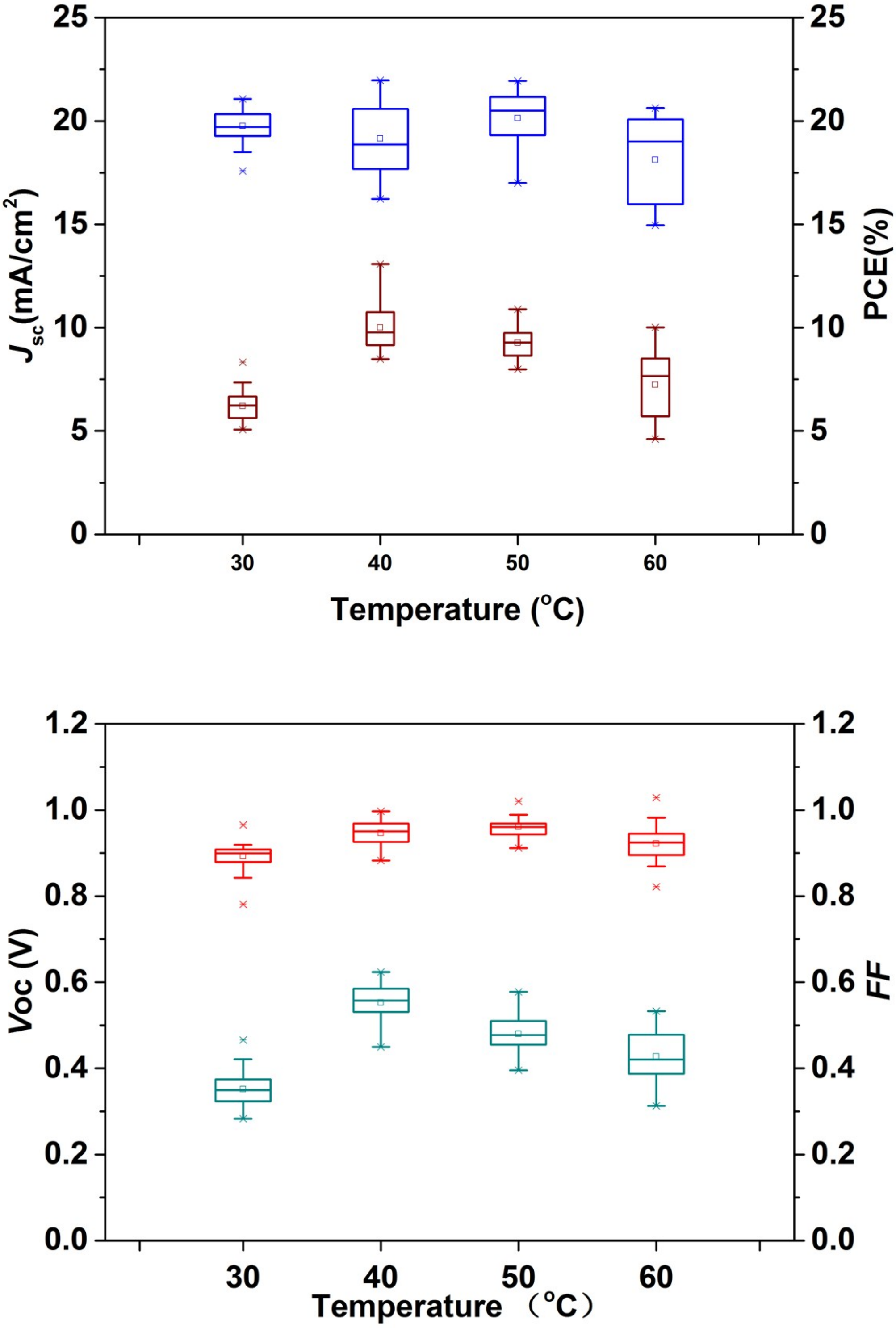

Figure S11 Photovoltaic parameters of perovskite solar cells based on pure PbI_2 prepared at different CH_3NH_3I spin-coating temperatures. Each box presents the parameter distribution of 40 devices under similar conditions.

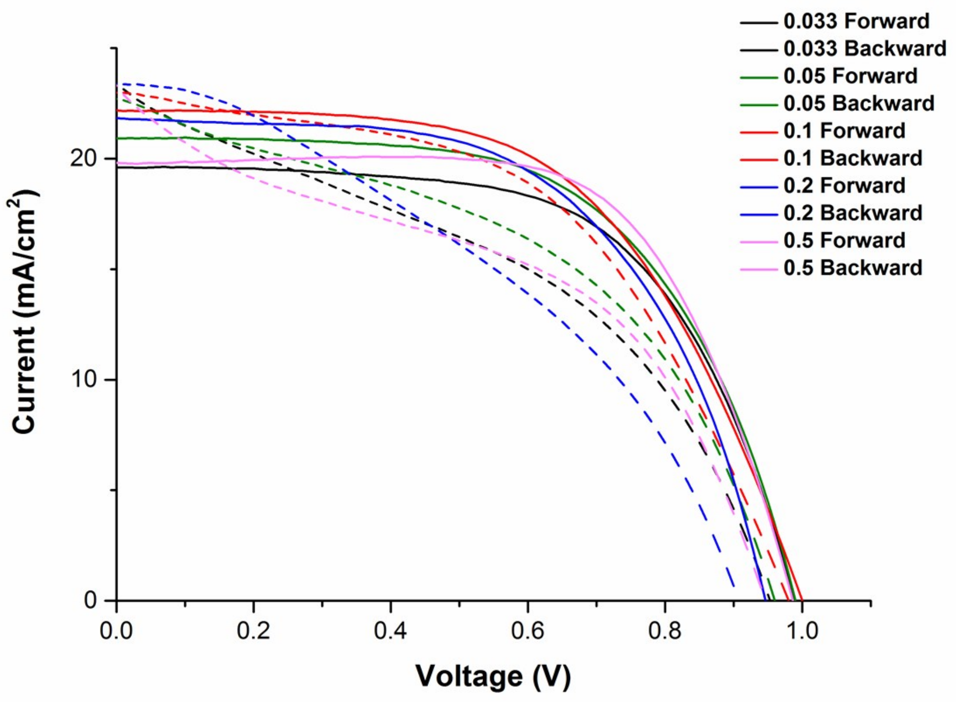

Figure S12 *J-V* plots of perovskite solar cells based on a 33% $PbCl_2$ molar ratio under different scanning speeds (V/s)

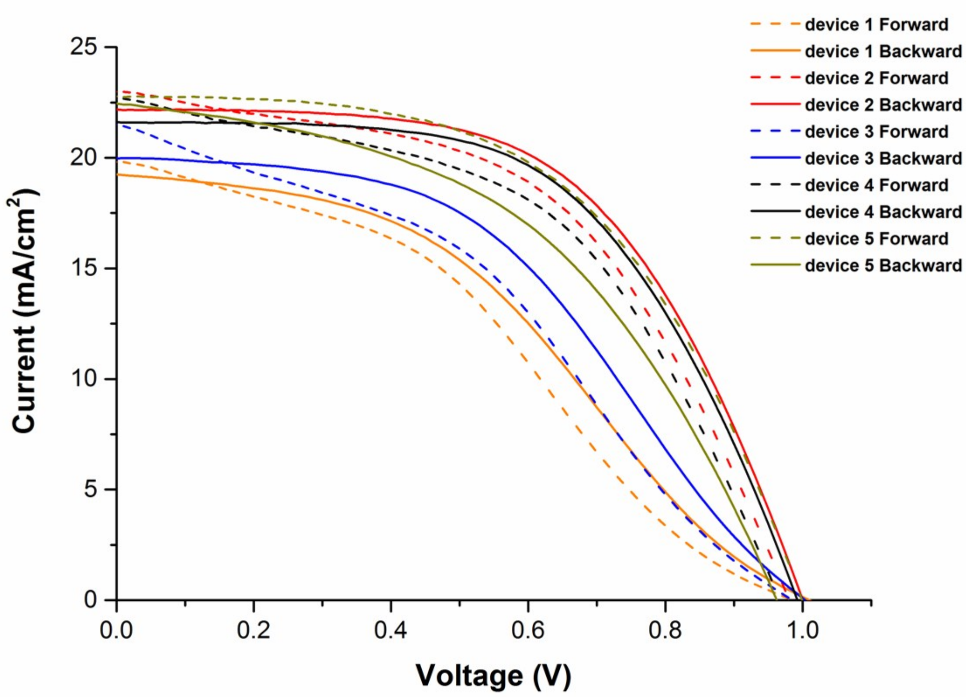

Figure S13 *J-V* plots of perovskite solar cells based on a 33% $PbCl_2$ molar ratio exhibiting different *PCE* values

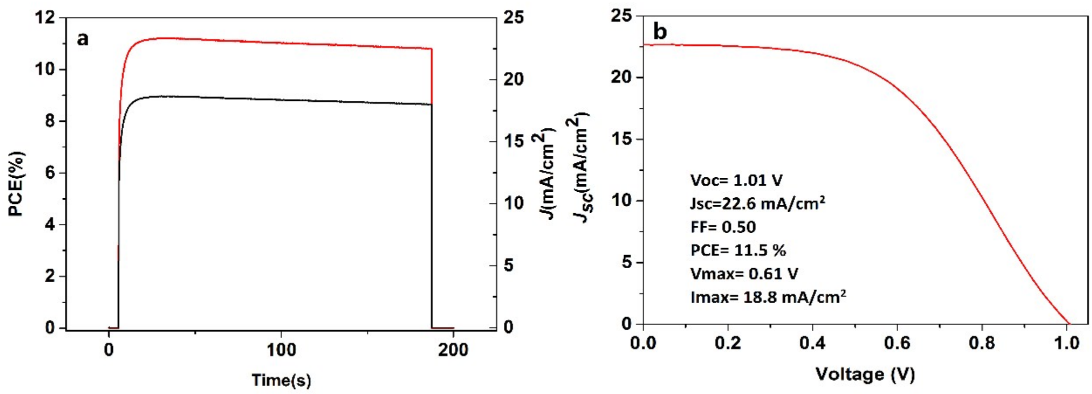

Figure S14 (a) J-V plots (b) PCE and J results of steady-state measurements

References:

1. M. M. Lee, J. Teuscher, T. Miyasaka, T. N. Murakami and H. J. Snaith, *SCIENCE*, 2012, **338**, 643-647.
2. W. Nie, H. Tsai, R. Asadpour, J. Blancon, A. J. Neukirch, G. Gupta, J. J. Crochet, M. Chhowalla, S. Tretiak and M. A. Alam, *SCIENCE*, 2015, **347**, 522-525.
3. Z. Xiao, Q. Dong, C. Bi, Y. Shao, Y. Yuan and J. Huang, *ADV MATER*, 2014, **26**, 6503-6509.
4. J. Burschka, A. Dualeh, F. Kessler, E. Baranoff, N. Cevey-Ha, C. Yi, M. K. Nazeeruddin and M. Grätzel, *J AM CHEM SOC*, 2011, **133**, 18042-18045.